Alkaline phosphatase-mediated hydrolysis of dissolved organic phosphorus enhances phosphorus cycling in the Yellow Sea☆

Xiaokun Ding [a,1], Haoyu Jin [b,c,1] , Chao Zhang [b,c,*] , Lei Lin [d] , Xinyu Guo [e] , Aobo Wang [f],
Jie Shi [b,c], Xiaohong Yao [b,c], Huiwang Gao [b,c]

[a] School of Ocean, Yantai University, Yantai, 264005, China
[b] Frontiers Science Center for Deep Ocean Multispheres and Earth System, and Key Laboratory of Marine Environment and Ecology, Ministry of Education of China, Ocean University of China, Qingdao, 266100, China
[c] Laboratory for Marine Ecology and Environmental Science, Qingdao Marine Science and Technology Centre, Qingdao, 266071, China
[d] College of Ocean Science and Engineering, Shandong University of Science and Technology, Qingdao, 266590, China
[e] Center for Marine Environmental Studies, Ehime University, Matsuyama, 790-8577, Japan
[f] School of Hydraulic and Civil Engineering, Ludong University, Yantai, 264025, China

ARTICLE INFO

ABSTRACT

The utilization of dissolved organic phosphorus (DOP) driven by alkaline phosphatase hydrolysis contributes significantly to mitigating coastal nitrogen pollution through alleviating phosphorus (P) limitation. However, the lack of a parameterization for this process limits the quantitative assessment of its impact on marine nutrient pollution and cycling. Our study addresses this issue using data from a series of on-board microcosm experiments conducted in the Yellow Sea, where P limitation prevails. In addition to incorporating the conventional temperature-dependent DOP decomposition, we improve this process by accounting for the effects of dissolved inorganic phosphorus (DIP) and dissolved inorganic nitrogen (DIN) on DOP utilization, based on well-established relationships among these variables. The improved model well reproduces nutrient dynamics observed during the incubations. Simulation results further indicate that DOP utilization can contribute up to 80% of bioavailable P in DIP-deficient environments. Without this process, DIP concentrations would decrease by over 50% within 2–5 days, leading to a 20%–60% decrease in chlorophyll *a* concentration and an approximately 100% increase in P turnover time. Moreover, the DOP-to-DIP conversion efficiency (i.e., DOP utilization rate) exhibits substantial spatiotemporal variability in surface seawater, with rates as high as 0.1 day^{-1} in the central Yellow Sea during spring and summer, and notable interannual variations with changes up to 0.1 day^{-1} from 2003 to 2019. This study establishes a parameterization scheme modeling the dynamics of DOP utilization rate, providing valuable insights into the transformation and ecological effects of organic phosphorus in coastal waters influenced by anthropogenic nitrogen pollution.

1. Introduction

In recent decades, many coastal regions worldwide have experienced severe phosphorus (P) deficiency relative to nitrogen (N), primarily due to multiple terrestrial N inputs such as riverine discharge and atmospheric deposition (Prasad et al., 2010; Malone and Newton, 2020; Li et al., 2024). The utilization of dissolved organic phosphorus (DOP) serves as a primary adaptive strategy for phytoplankton to cope with P

deficiency (Wang et al., 2011; Liang et al., 2022; Su et al., 2023). In P-deficient environments, planktonic cells synthesize alkaline phosphatase (AP) to hydrolyze DOP into dissolved inorganic phosphorus (DIP), thereby increasing the availability of organic phosphorus (Lin et al., 2016; Jin et al., 2024). Evidence suggests that DOP utilization can account for as much as 90% of the bioavailable P in the open ocean (Karl, 2014). In nutrient-rich coastal waters, although DIP stocks are much higher than in open oceans, the deficiency of DIP relative to

dissolved inorganic N (DIN) makes DOP utilization become the potential source of bioavailable P (Duhamel et al., 2021; Liang et al., 2022). A recent study demonstrates that phytoplankton can absorb substantial and even excess DIN for growth through enhancing DOP utilization in coastal waters, i.e., Anthropogenic N Pump (Jin et al., 2024). Globally, the overall decomposition rate of DOP (including DOP utilization and other mineralization processes) is twice that of other dissolved organic compounds including carbon and nitrogen (Duhamel et al., 2021). Increasing attention is being directed toward understanding the role of DOP utilization and its implications for biogeochemical cycles in seawater (Chu et al., 2018; Jin et al., 2024).

Various environmental factors influence the rate of DOP utilization by regulating alkaline phosphatase activity (APA). Numerous studies have highlighted the significant stimulation of APA by low DIP concentrations (Dyhrman and Ruttenburg, 2006; Lomas et al., 2010; Lin et al., 2016). APA is generally inversely correlated with DIP levels, and inducible AP becomes activated when DIP concentrations drop below a specific threshold (Suzumura et al., 2012; Mahaffey et al., 2014). This DIP threshold varies considerably across different coastal waters due to variations in nutrient levels and phytoplankton communities. For instance, APA reaches high levels when DIP concentration falls below 0.03 mmol m^{-3} in the northern Adriatic Sea (Ivančić et al., 2016), while in Daya Bay, a noticeable increase in APA occurs at a DIP threshold of 0.20 mmol m^{-3} (Zhang et al., 2018). In the Yellow Sea, the DIP threshold has been reported as 0.02 mmol m^{-3} (Jin et al., 2024). Atmospheric deposition and riverine input significantly stimulate the DOP utilization in coastal seas by depleting DIP due to increasing N concentrations (Rees et al., 2009; Jin et al., 2024). Additionally, factors such as seawater temperature and the availability of iron and zinc can also influence APA (Ruttenberg et al., 2012; Browning et al., 2017). The complexity of coastal environments hinders the effective development of parameterization schemes for calculating DOP utilization rates by marine ecological models.

Marine ecological models, developed from field observations and experiments, can simulate the dynamic variations of biogeochemical processes, serving as valuable tools for quantitatively analyzing marine processes (Shukla et al., 2021; Gao et al., 2022). Most marine ecological models are structured around the conversion between nutrients, phytoplankton, zooplankton, and detritus, and are primarily used to analyze changes in inorganic nutrients and primary production processes (Fennel et al., 2006; Fan and Song, 2014; Zhang et al., 2019; Fang et al., 2022). Enhanced ecological models have been applied to investigate issues such as nitrous oxide emissions, hypoxia, and iron cycling (Yoshikawa et al., 2015; Zhou et al., 2017; Xiu and Chai, 2021; Yu et al., 2021). Despite these advancements, the role of DOP utilization in ecological simulation has not received sufficient attention, and DOP is often not considered a state variable. This is largely because traditional models focus on inorganic nutrients, treating DOP primarily as an intermediate pool between particulate organic P and DIP, rather than a direct contributor to primary production (Laurent et al., 2012; Yu et al., 2021). However, as P limitation becomes increasingly common in coastal waters, DOP utilization plays a more critical role in sustaining phytoplankton growth and should be explicitly represented in biogeochemical models.

Some ecological models have integrated DOP utilization, but their calculated methods are often oversimplified. For example, the utilization rate of DOP has been set as a fixed empirical constant when modelling its effect on phytoplankton growth in the Mediterranean Sea (Llebot et al., 2010). Letscher et al. (2022) highlighted the significant contribution of DOP to net community production using an inverse P-cycling model, replacing the global oceanic annual DOP utilization rate with nine fixed constants. Chu et al. (2018) attempted to simulate DOP transformation based on a constant P principle, fixing the DIP limiting factor at 0.3 when the DIP concentration falls below 0.03 mmol m^{-3}. Overall, the parameterization of DOP utilization remains underdeveloped in current ecological models, failing to capture the dynamic

variations of DOP utilization, and thus hindering the quantitative analysis of its contributions to nutrient cycling and primary production at high spatiotemporal resolution.

The Yellow Sea, a shallow marginal sea off the eastern coast of China with a mean depth of approximately 44 m (Fig. 1), has experienced a significant P deficiency due to continuous terrestrial N inputs (Moon et al., 2021; Zhong and Ran, 2024). This pronounced P deficiency creates conditions that can trigger DOP utilization (Mahaffey et al., 2014; Lin et al., 2016), making the Yellow Sea a favorable environment to study the impact of DOP utilization on P cycling in coastal waters. In this study, we conducted a series of on-board incubation experiments in the Yellow Sea to address key knowledge gaps regarding DOP utilization dynamics. Specifically, we aimed to develop an improved parameterization scheme that incorporates the effects of environmental factors on DOP utilization, thereby enhancing the predictive accuracy of ecological models. The findings provide a quantitative assessment of DOP utilization and its impact on nutrient cycling, offering insights into mitigating P limitation and maintaining ecosystem stability in anthropogenically impacted coastal waters.

2. Materials and methods

2.1. On-board microcosm experiments

Four on-board microcosm experiments were conducted at three stations in the Yellow Sea during the summer (July–August) cruise in 2018 and spring (March–April) and summer cruises in 2019, respectively, aboard the R/V Dongfanghong 2 and R/V Beidou (Fig. 1). Surface seawater (3–5 m depth) was collected from three stations, designated as Y1, Y2, and Y3. Additionally, seawater collected from the deep chlorophyll *a* (Chl-a) maximum layer at station Y1 was labeled as Y1$_{DCM}$.

The collected seawater was transferred into acid-washed polycarbonate bottles (20 L, Nalgene 2251-0050) after filtration through a 200 μm acid-washed nylon mesh. To estimate the impact of increasing N concentrations on DOP utilization, N-rich aerosol extracts were immediately added to simulate different atmospheric deposition scenarios. Atmospheric aerosols were collected from the Atmospheric Environment Monitoring Station at the Laoshan campus of Ocean University of China, Qingdao, China (36.16° N, 120.50° E). Low, medium, and high concentrations of aerosol additions were performed at all stations, except at Y1 and Y1$_{DCM}$ where the medium concentration was not applied (Fig. 1; Table A1). After aerosol addition, the bottles were placed in three microcosm tanks and incubated for 4–6 days for 20 L experiments. Flow-through surface seawater was used to maintain a stable temperature, closely resembling in-situ conditions.

During the microcosm experiments, water temperature, light intensity, DIN, DIP, dissolved silicate (DSi), Chl-a concentrations, and APA were measured every 24 h. Concentrations of particulate organic carbon, total dissolved phosphorus, and DOP were measured at the beginning and end of the incubations. Detailed protocols for incubation experiments, aerosol collection, and sample measurement methods can be found in Jin et al. (2024).

2.2. Numerical simulation

An ecological box model was used to estimate the impact of DOP utilization on P cycling. As shown in Fig. A1, the model includes 13 state variables: two forms of DIN (nitrate and ammonium), DIP, DSi, dinoflagellate, diatom, microzooplankton, mesozooplankton, dissolved organic nitrogen, DOP, particulate organic nitrogen, particulate organic phosphorus, and biogenic silica. This selection of state variables ensures that key processes of nutrient cycling, particularly those related to DOP production, transformation, and utilization, are accurately represented. The model is based on the NPZD (Nutrient-Phytoplankton-Zooplankton-Detritus) framework, which has been extended to include organic nutrient pools and nutrient cycling for a more comprehensive
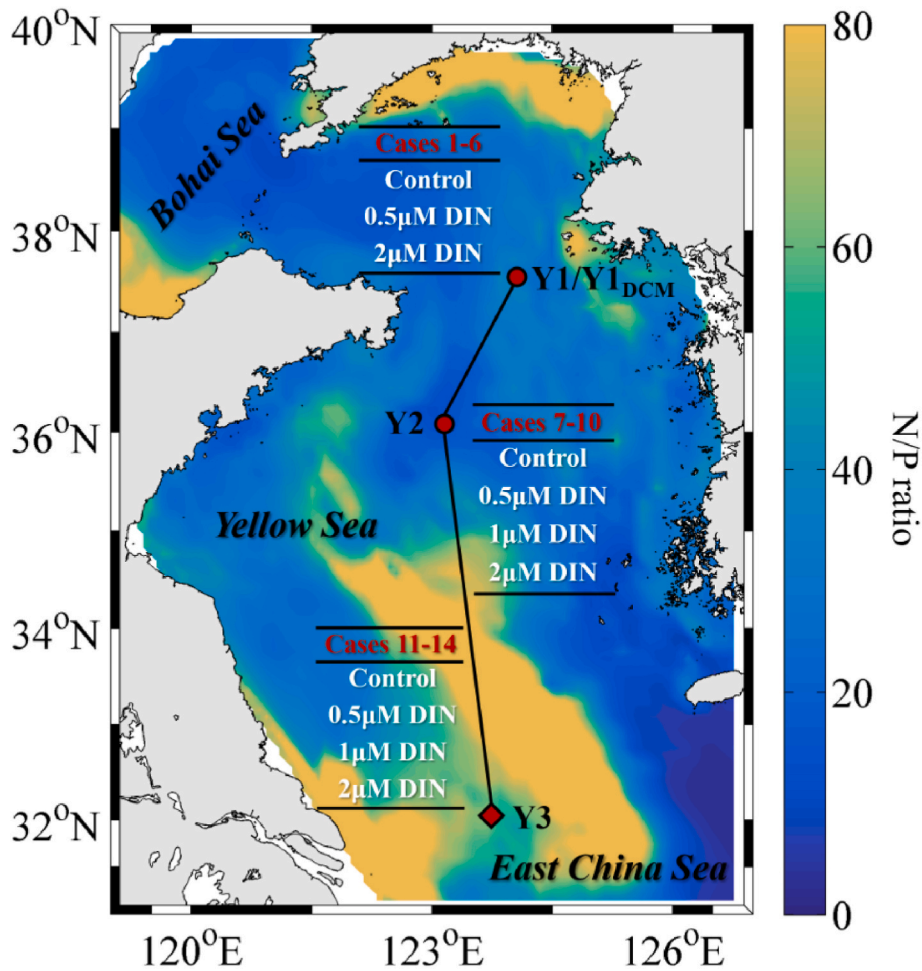
Fig. 1. Seawater sampling stations for the microcosm experiments. Experiment for the deep chlorophyll *a* maximum layer at Y1 is labeled as Y1$_{DCM}$. At four stations, 14 microcosm experiments were conducted, including control groups and treatments with atmospheric aerosol additions containing varying DIN concentrations. These experiments also formed the basis for numerical simulations under corresponding scenarios. The background color indicates the DIN-to-DIP ratio, sourced from Liu et al. (2022). (For interpretation of the references to colour in this figure legend, the reader is referred to the Web version of this article.)

representation of coastal ecosystems. A detailed description of the model can be found in Ding et al. (2021). In this study, a new parameterization scheme for DOP utilization (Section 3.1) was developed based on experimental data to replace the simplified calculation of the DOP decomposition rate in the original model.

The box model was initialized using data from the first day of incubation experiments. It was then run to simulate the daily variation of nutrient cycling across 14 experimental scenarios, driven by observed daily temperature and light intensity. The values of all biological parameters are provided in Table A2. To assess the ecological impact of DOP utilization, an additional 14 numerical experiments were conducted in which the DOP utilization rate was set to zero. Following these two series of simulations, the effects of DOP utilization on DIN concentration, Chl-a concentration, and phosphorus turnover time (PTime) were calculated:

$$R_{DIP} = (DIP_{none} - DIP_c) / DIP_c \tag{1}$$

$$R_{Chl} = (Chl_{none} - Chl_c) / Chl_c \tag{2}$$

$$R_{PTime} = (PTime_{none} - PTime_c) / PTime_c \tag{3}$$

$$PTime = C_{DIP} / PHYP_{ass} \tag{4}$$

where R_{DIP}, R_{Chl}, and R_{PTime} represent the change in DIP, Chl-a, and PTime, respectively, when the DOP utilization process is excluded; DIP_c,

Chl_c, and $PTime_c$ denote DIP concentration, Chl-a concentration, and PTime in control groups, while DIP_{none}, Chl_{none}, and $PTime_{none}$ represent the corresponding values in the simulations without DOP utilization; C_{DIP} represents the concentration of DIP, and $PHYP_{ass}$ denotes the assimilation rate of DIP by phytoplankton. In addition, to estimate the impact of DOP utilization on the N cycle, the N turnover time (NTime) was also calculated:

$$NTime = C_{DIN} / PHYN_{ass} \tag{5}$$

where C_{DIN} represents the concentration of DIN, and $PHYN_{ass}$ is the assimilation rate of DIN by phytoplankton.

2.3. Data source

To evaluate the spatial-temporal variation of DOP utilization rate in the Yellow Sea, monthly data of DIN and DIP in surface water from 2003 to 2019 were collected from the outputs of a machine-learning model (Liu et al., 2022). Additionally, monthly sea surface temperature (SST) data at a 4-km resolution from the Moderate Resolution Imaging Spectroradiometer (MODIS) were obtained from the NASA Ocean Color website (http://oceancolour.gsfc.nasa.gov).

3. Results and discussion

3.1. Parameterization scheme of DOP utilization

The DOP utilization rate was defined as the ratio of APA to DOP concentration, representing the potential conversion efficiency of existing DOP within a given timeframe. Experimental data demonstrate a significant inverse relationship between the DOP utilization rate and the DIP concentration (Fig. 2a). A distinct DIP threshold of 0.02 mmol m^{-3} is observed, below which reductions in DIP concentration result in a rapid increase in DOP utilization rate, while the rate remains relatively low when DIP concentration exceeds this threshold. Under conditions of low DIP concentration, phytoplankton synthesize large amounts of alkaline phosphatase, enhancing APA and thereby stimulating DOP utilization (Ghyoot et al., 2015; Lu et al., 2021). Consequently, low DIP concentration is considered a critical factor influencing DOP utilization.

Previous studies suggest that high DIN concentrations can intensify the consumption of DIP and have a positive effect on APA (Anthropogenic N Pump, Jin et al., 2024). However, correlation analyses incorporating all experimental data indicate that there was no significant relationship between DOP utilization rate and DIN concentration in our study (Fig. 2b). A significantly positive correlation between DOP utilization rate and DIN concentration was observed only when DIP concentrations were below 0.02 mmol m^{-3} (Fig. 2c–d). This suggests the following two points: first, low DIP concentration is a key factor that determines the changing pattern of DOP utilization rate; second, once DIP concentration decreases to a certain threshold, the extra supply of DIN can further enhance the utilization rate of DOP. However, the influence of DIN on DOP utilization under high phosphorus conditions remains complex. Studies have shown that even at relatively high DIP concentrations, an increase in nitrogen concentration can still stimulate APA (Neddermann and Nausch, 2005; Rees et al., 2009; Fitzsimons et al., 2020; Jin et al., 2024). These discrepancies indicate that the effect of nitrogen on DOP utilization is not solely dependent on DIP concentration but may also be influenced by phytoplankton community

composition, ambient temperature, and other biogeochemical factors (Rees et al., 2009; Fitzsimons et al., 2020; Zhou et al., 2021). Therefore, further research is needed across different ecosystems and nutrient conditions to fully elucidate the role of nitrogen in DOP utilization.

Phytoplankton are considered one of the major contributors to AP production in aquatic environments (Lin et al., 2016). Numerous studies have shown that P deficiency relative to N favors the proliferation of harmful algae in coastal waters, due to their capacity of enhancing APA (Chen and Liu, 2010; Wang et al., 2022). Jin et al. (2024) emphasized the positive effect of elevated Chl-a/DIP ratios on the surge of APA. However, our experimental data reveal a slight negative correlation between the DOP utilization rate and Chl-a concentration ($R^2 = 0.14$, $p < 0.05$, Fig. A2), which has also been observed in other coastal seas (Davies and Smith, 1988), suggesting the limited control of Chl-a on the conversion efficiency of DOP. This inconsistency may arise under P-deficient conditions, where increasing DIP levels can have contrasting effects on phytoplankton growth and DOP utilization. Elevated DIP concentrations can stimulate phytoplankton growth by alleviating P limitation while reducing DOP utilization, since APA enhancement is typically triggered by low DIP levels (Mahaffey et al., 2014; Lin et al., 2016). This leads to a decrease in the DOP-to-DIP conversion rate, which inhibits the recycling of P from DOP and reduces DOP utilization.

As described above, we preliminarily propose a parameterization scheme for the DOP utilization rate, by integrating the effects of DIN and DIP on DOP utilization observed in this study (Fig. 2):

$$[APA / DOP] = \begin{cases} \left(k_1 DIP^{-1.29} + k_2 DIN \right) \bullet \exp\left(k_3 T\right) & DIP \leq 0.02\, mmol \bullet m^{-3} \\ k_4 DIP^{-1.29} \bullet \exp\left(k_3 T\right) & DIP > 0.02\, mmol \bullet m^{-3} \end{cases}$$

$$(6)$$

where the fitting coefficients k_1, k_2, and k_4 were assigned values of 0.00019, 0.63, and 0.0054, respectively. The effect of water temperature (T) was incorporated into the scheme, given its significant influence on biochemical processes (Eppley, 1971; Kremer et al., 2017), following the Eppley curve with a coefficient k_3 of 0.0693 (Yoshikawa et al., 2005; Fennel et al., 2006; Fan and Song, 2014). The accuracy of the fitting
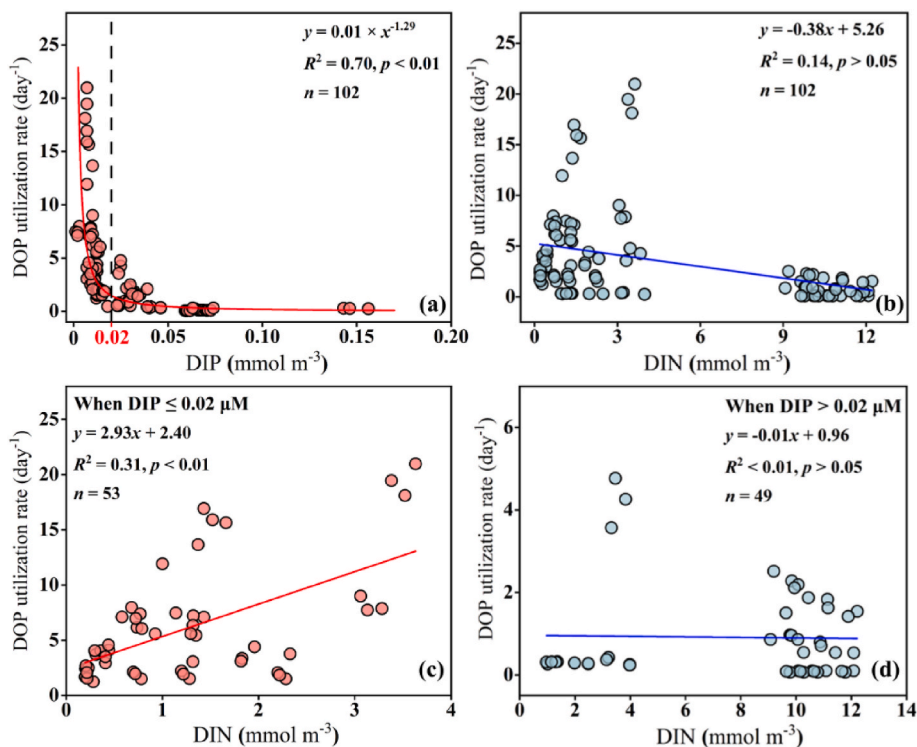
Fig. 2. Relationship between DOP utilization rate and concentration of (a) DIP, (b) DIN, (c) DIN (where DIP ≤0.02 mmol m^{-3}), and (d) DIN (where DIP >0.02 mmol m^{-3}).

equation (Eq. (6)) was validated through significance testing ($p < 0.05$) using experimental data. Additionally, the conventional measurement of APA is based on 4-methylumbelliferyl phosphate as the only DOP source (Hoppe, 1983), which may overestimate the actual DOP utilization rate considering the complexity of DOP in realistic conditions. Moreover, the DOP utilization rate is generally difficult to determine accurately due to the continuous synthesis and decomposition processes of DOP over diurnal cycles. Previous studies suggested that the DOP decomposition rate is approximately 0.01–0.28 day^{-1} in coastal waters based on the time-series approach using replicated incubation bottles in total darkness (Benitez-Nelson, 2000; Hopkinson et al., 2002; M. Nausch and G. Nausch, 2006). Some ecological models have used similar empirical constants for the DOP decomposition rate (Llebot et al., 2010; Letscher et al., 2022). Consequently, an empirical correction was applied to the calculated APA/DOP ratio to estimate the actual DOP utilization rate:

$$Rate\ of\ DOP\ utilization = k_c[APA\ /\ DOP] \qquad (7)$$

where the correction coefficient k_c was set to 0.004 (details can be seen in the next paragraph) to ensure that the calculated DOP utilization rates are in the range reported in previous studies. This adjustment is essential for developing biochemical process parameterization schemes, as measuring ecological parameters directly remains challenging (Yoshikawa et al., 2005; Ding et al., 2021).

Sensitivity numerical experiments were conducted to examine how nutrient cycling varied in response to changes in k_c. The predicted state variables for the sensitivity analysis were represented by the mean nutrients and Chl-a concentration over the entire simulation period. Using a k_c of 0.004 as the control, k_c was increased and decreased by 50% in each sensitivity experiment. The sensitivity of the predicted state variables to k_c was quantified using the factor $S(F) = \left| \frac{\Delta F/F}{\Delta k_c/k_c} \right|$, where F represents the concentration of DIN, DIP, DSi, or Chl-a. Here, ΔF represents the variation in F corresponding to the change (Δk_c) in the parameter k_c. As shown in Table A3, the sensitivity factors for all 14 groups were less than 0.4, indicating that the calculated results were robust to variations in k_c.

3.2. Impact of DOP utilization on P cycling

The ecological model, incorporating the newly established parameterization scheme for DOP utilization, successfully replicated the nutrient cycling observed in all 14 incubation experiments (Figs. A3–A6). Notably, the new parameterization scheme can dynamically simulate changes in DOP utilization rates in response to variations in nutrient concentration. As shown in Table 1, the DOP utilization rate

Table 1
Rate of DOP utilization in simulations of the control group (Control), low addition group (Low), medium addition group (Middle), and high addition group (High) of atmospheric aerosols.

Station	Treatment	Range (day^{-1})	Average (day^{-1})
Y1	Control	0.019–0.022	0.020
	Low	0.031–0.036	0.033
	High	0.041–0.046	0.044
Y1$_{DCM}$	Control	0.003–0.005	0.004
	Low	0.003–0.007	0.004
	High	0.003–0.006	0.004
Y2	Control	0.007–0.009	0.008
	Low	0.010–0.012	0.011
	Middle	0.014–0.019	0.018
	High	0.023–0.032	0.028
Y3	Control	0.007–0.013	0.016
	Low	0.005–0.043	0.018
	Middle	0.006–0.042	0.022
	High	0.006–0.044	0.024

varies significantly across different scenarios. For example, the DOP utilization rate at station Y1 ranges from 2.0% to 4.4% per day, significantly higher than at station Y1$_{DCM}$ (0.4% per day). Additionally, aerosol additions at all stations increased the DOP utilization rate. Similarly, studies in other regions have also reported large variations in DOP utilization rates, sometimes differing by more than two orders of magnitude (Björkman et al., 2018; Bell et al., 2020). However, the complexity of environmental factors makes it challenging to establish precise quantitative relationships for assessing DOP utilization (Lin et al., 2016; Nausch et al., 2018; Duhamel et al., 2021). Our findings demonstrate the superiority of the new DOP utilization parameterization scheme, highlighting the limitations of using a fixed empirical constant for the DOP decomposition rate in previous models. These simulation results enable further quantitative analysis of the ecological impacts of DOP utilization.

3.2.1. Influence on DIP concentration

DOP utilization is regarded as a significant source of DIP in the Yellow Sea (Jin et al., 2021). Simulations for stations Y1 and Y3 show that the DIP production rate from DOP utilization is substantially higher than that from particle decomposition and plankton metabolism (Fig. A7). According to Fig. 3a, DOP utilization can contribute up to 80% of the total DIP sources at stations Y1 and Y3. At station Y2, DOP utilization accounted for 20%–60% of the DIP source. Consequently, excluding DOP utilization can lead to a significant decrease (24%–65%) in DIP concentration within a few days at stations Y1, Y2, and Y3 (Fig. 3b). However, at station Y1$_{DCM}$, DOP utilization contributed less than 20% of the DIP source (Fig. 3a2). No significant change in DIP concentration was observed at station Y1$_{DCM}$ when DOP utilization was excluded, likely due to the relatively high DIP stock (Fig. A4b). Aerosol addition can amplify the impact of DOP utilization on DIP by increasing its rate, highlighting the significant role of the "Anthropogenic N Pump" (Jin et al., 2024). DOP utilization has also become an important P nutrient source in many other coastal seas worldwide. For example, studies have shown that DOP supplied 40%–70% of P nutrients in the offshore Northwest Atlantic Ocean (Diaz et al., 2018), and up to 82% in the Sargasso Sea (McLaughlin et al., 2013).

3.2.2. Influence on Chl-a concentration

DIP concentration is the main limiting factor for phytoplankton growth in the Yellow Sea (Moon et al., 2021). At stations Y1 and Y2, surface Chl-a concentrations could decrease by about 20%–60% within several days if DOP utilization is excluded (Fig. 3c). DOP utilization enhances primary productivity by supplying DIP, a crucial nutrient for phytoplankton growth (Wang et al., 2022; Jin et al., 2024). Studies have found that DOP utilization accounted for 25% of primary production in the Sargasso Sea (Lomas et al., 2010) and facilitated primary productivity recovery within 48 h in the DIP-deficient Mediterranean Sea (Sisma-Ventura and Rahav, 2019). Letscher and Moore (2015) have also found that DOP utilization can enhance net primary productivity by 10% in the global ocean, and a recent study suggests that about 15% of global marine net primary productivity is supported by autotroph-driven DOP utilization (Shen and Wang, 2025), highlighting the crucial role of DOP utilization in global marine primary production. Additionally, aerosol additions can further influence Chl-a concentrations by accelerating DOP utilization. At station Y1$_{DCM}$, the high DIP stock resulted in a minimal impact of DOP utilization on Chl-a concentration. At station Y3, Chl-a concentration began to decrease slightly from the third day onward if DOP utilization was excluded, due to a drop in DIP concentration to around the threshold value of 0.02 mmol m^{-3} (Fig. A4d).

Currently, with the widespread input of N-containing substances from terrestrial sources globally, phytoplankton growth in coastal areas is limited by low DIP concentrations (Laurent et al., 2012; Ding et al., 2021). Our simulations indicate that the addition of N-containing nutrients could double primary productivity by stimulating DOP utilization
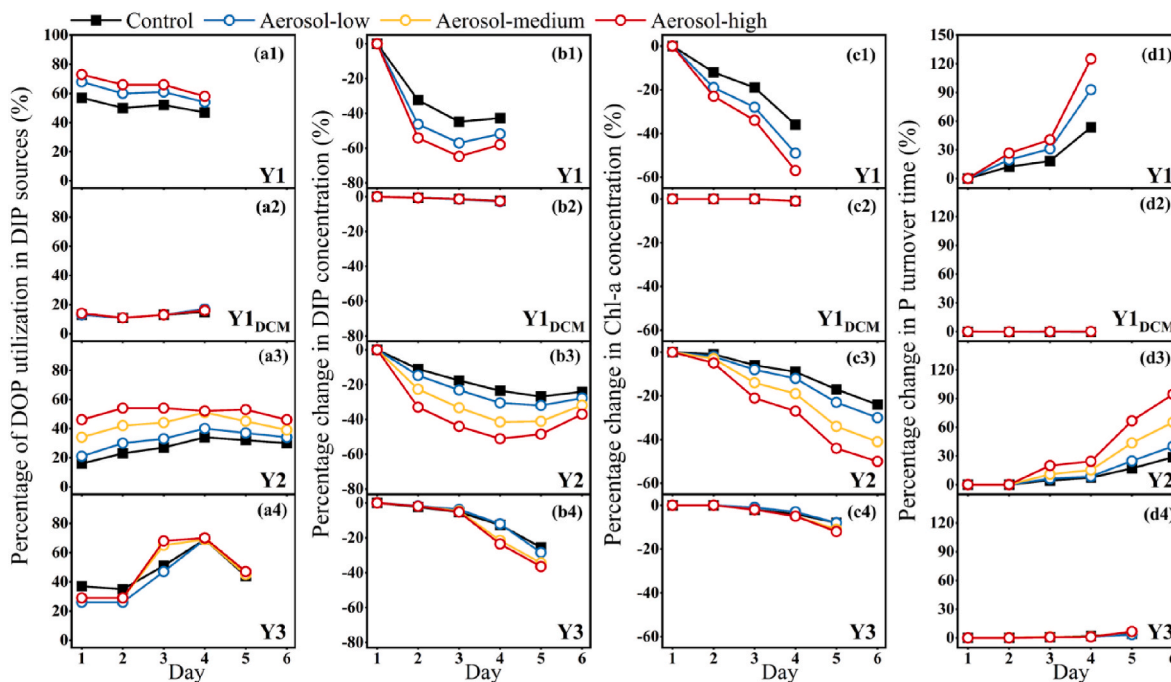
Fig. 3. Simulated influence of DOP utilization on P cycling. Negative values correspond to the decreasing value of the variable after excluding the DOP utilization in the simulation.

(Figs. A7a and c). If DOP utilization is excluded, the high nutrient addition group showed a ~30% lower Chl-a concentration compared to the no-addition group (Fig. 3c). Without DOP utilization, the nutrient structure in coastal areas with high N-to-P ratios could become further imbalanced, leading to a rapid decline in Chl-a concentration over time, eventually transforming the area into a low-productivity environment.

3.2.3. Influence on P turnover rate

Rapid P turnover rates within dissolved and particulate pools suggest that even low P concentrations can sustain relatively high primary production (Benitez-Nelson and Buesseler, 1999). In this study, we use DIP turnover time to represent the P cycling rate, calculated as described in Eq. (4). As shown in Fig. A8d, PTime ranges from approximately 0.3 days–9.2 days in the Yellow Sea, consistent with values reported in previous studies of coastal waters (Benitez-Nelson, 2000; Zhang and Yin, 2007). Aerosol additions can reduce PTime by up to 35% within a few days, highlighting the significant impact of terrestrial N inputs on coastal P cycling. A longer PTime was observed when the DOP utilization process was excluded in the model (Fig. A8c1&c3). As shown in Fig. 3d, excluding DOP utilization in seawater could result in a 130% increase in PTime at station Y1 and a 90% increase at station Y2 over the following days, particularly in the high aerosol addition group. These findings provide new insights into the quantitative role of DOP utilization in accelerating P cycling in P-limited marine environments. The impact of DOP utilization on P turnover is minimal at DIP-sufficient stations $Y1_{DCM}$ and Y3.

On the other hand, DOP utilization also significantly affects N cycling. Excluding DOP utilization could increase DIN concentrations by 20% at station Y1 and by 60% at station Y2 (Fig. A10a). Without DOP utilization, NTime would more than double, especially in the high addition group at station Y1, where it would increase over fivefold. Therefore, in P-deficient environments, DOP utilization can significantly increase DIN assimilation rate by providing DIP, thereby accelerating N cycling. However, the impact of DOP utilization on N cycling at stations $Y1_{DCM}$ and Y2 is relatively weak (Fig. A10), due to its limited influence on phytoplankton growth (Fig. 3c). Furthermore, NTime varies significantly due to regional differences in DIN stocks and phytoplankton

growth conditions (Fig. A10c; Middelburg and Nieuwenhuize, 2000; Cheung et al., 2022). Studies on the global ocean have suggested that DOP utilization enhances N fixation capacity by 26%, while the N fixation rate would decrease by 9% without DOP utilization (Letscher and Moore, 2015; Shen and Wang, 2025). These findings support our assertion that DOP utilization can stimulate the marine nutrient cycling.

3.3. Spatial-temporal variation of DOP utilization rate

Using collected data on nutrient concentrations and SST, the newly established parameterization scheme (Eq. (7)) was applied to calculate the DOP utilization rate in the Yellow Sea. Fig. 4 shows that the DOP utilization rate is significantly higher in spring and summer compared to autumn and winter. In June, a high-value zone of approximately 0.1 day^{-1} emerged in the central region of the southern Yellow Sea. The high DOP utilization zones in spring and summer predominantly coincided with areas where DIP concentrations were below 0.02 mmol m^{-3} (Fig. A11), highlighting the crucial role of low DIP levels in controlling DOP utilization. However, in the southwestern coastal waters of the Yellow Sea, the DOP utilization rate was below 0.001 day^{-1} in summer (Fig. 4g–i), likely due to the inhibitory effect of DIP inputs from coastal river inflows (Figs. A12g–A12i; Fan and Song, 2014). During autumn and winter, intensified vertical mixing in the seawater increases DIP concentrations (Zhu et al., 2018; Ding et al., 2021). Phytoplankton acquire P nutrients more efficiently by directly absorbing DIP, leading to a significant reduction in the DOP utilization rate. The occurrence of low DOP utilization rates alongside high DIN concentrations or temperatures (Figs. A12–A13) suggests that the influence of temperature and DIN on DOP utilization might be limited.

We also calculated the interannual variation in DOP utilization rate for each month from 2003 to 2019 (defined as the difference between maximum and minimum values, Fig. 5). In spring and summer, the range of DOP utilization rates was relatively large across most areas of the Yellow Sea, especially in June, with values in the southern Yellow Sea reaching nearly 0.1 day^{-1}. The southwestern offshore region also showed significant interannual variability in DOP utilization rates, primarily due to substantial fluctuations in estuarine nutrient conditions
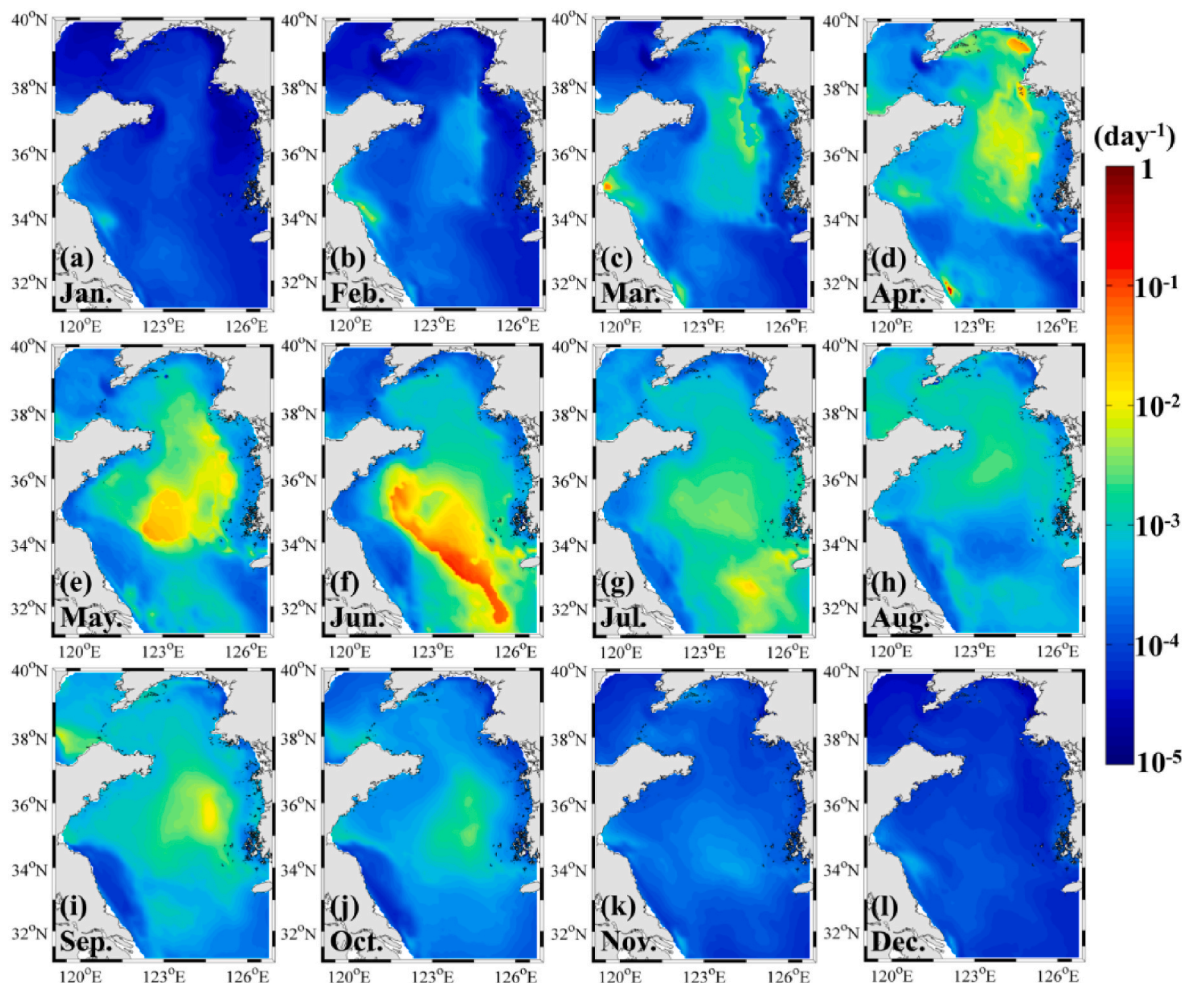
Fig. 4. Monthly variations of DOP utilization rate in surface water.

from riverine inputs (Wang et al., 2018). In contrast, the interannual variation in DOP utilization rates during winter was minimal, as rates remained consistently low (<0.003 day⁻¹, Fig. 4). Coastal seas often experience significant spatiotemporal variations in DIP concentrations and other environmental factors due to climate change and terrestrial inputs, particularly during the peak period of phytoplankton growth in spring and summer (Zhang et al., 2019; Ding et al., 2024). These variations can lead to substantial spatiotemporal changes in DOP utilization rates. The significant temporal and spatial variability in DOP utilization rates has been documented in numerous studies, yet a systematic quantitative analysis has yet to be conducted (Hung et al., 2003; Ruttenberg and Dyhrman, 2005; Casey et al., 2009; Björkman et al., 2018). Collectively, our study provides a parameterization of DOP utilization and highlights its key role in affecting biogeochemical cycles and primary productivity in coastal waters (Fig. 6).

3.4. Uncertainty and implication for other coastal seas

Traditional long-term dark incubation experiments have been widely used to estimate DOP utilization rates by minimizing light-driven DOP production (Hopkinson et al., 2002; M. Nausch and G. Nausch, 2006). However, these methods are time-consuming, labor-intensive, and difficult to scale, limiting their ability to capture the dynamic nature of DOP utilization in coastal ecosystems. As a result, available experimental data remain scarce. In the Middle Atlantic Bight, Hopkinson et al. (2002) reported DOP utilization rates ranging from 0.01 day⁻¹ to 0.20 day⁻¹ during spring and summer, while in the Baltic Sea, rates of

0.04–0.28 day⁻¹ were observed from May to July (M. Nausch and G. Nausch, 2006). In contrast, direct experimental measurements of DOP utilization rates are currently lacking for China's coastal waters, where APA is commonly used as a proxy for DOP turnover (Wang et al., 2014; Ou et al., 2018). The parameterization scheme developed in this study estimated DOP utilization rates in the Yellow Sea ranging from 0.01 day⁻¹ to 0.14 day⁻¹ during spring and summer, which aligns well with previous findings from other coastal regions.

Although on-board microcosm experiments provide a controlled environment for investigating biogeochemical processes, they also have inherent limitations. Boundary effects and confinement within incubation bottles may alter phytoplankton growth dynamics and nutrient availability, potentially affecting the extrapolation of experimental results to natural ecosystems. In this study, we took several measures to mitigate these limitations, including the use of low-adsorption polycarbonate bottles, daily manual agitation to prevent stratification, and large-volume incubations to minimize confinement effects. Additionally, natural light and temperature conditions were maintained using a photomask and a flow-through seawater system, ensuring that experimental conditions closely resembled those in situ (Jin et al., 2024).

In contrast, in situ experiments provide the advantage of capturing real-time interactions between phytoplankton and their surrounding environment. However, these measurements are often subject to high variability due to hydrodynamic mixing, which can obscure the specific role of DOP utilization. The controlled conditions of our microcosm experiments ensured stable environments necessary for parameterizing DOP utilization rates while eliminating confounding effects from
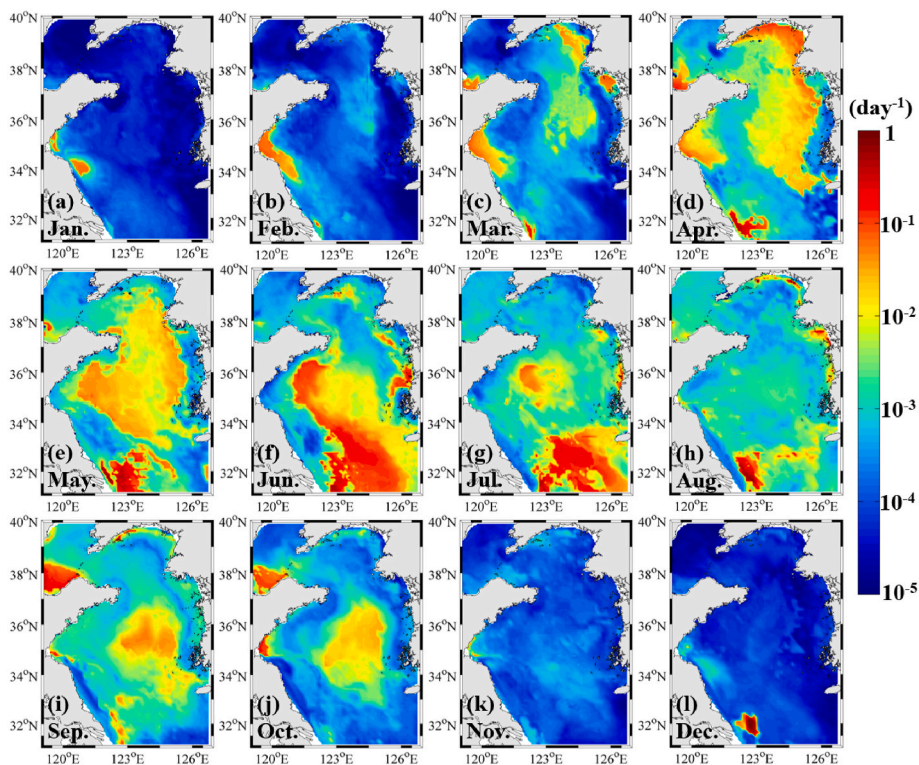
Fig. 5. Monthly range (maximum minus minimum) of DOP utilization rates in surface water from 2003 to 2019, showing interannual variability.
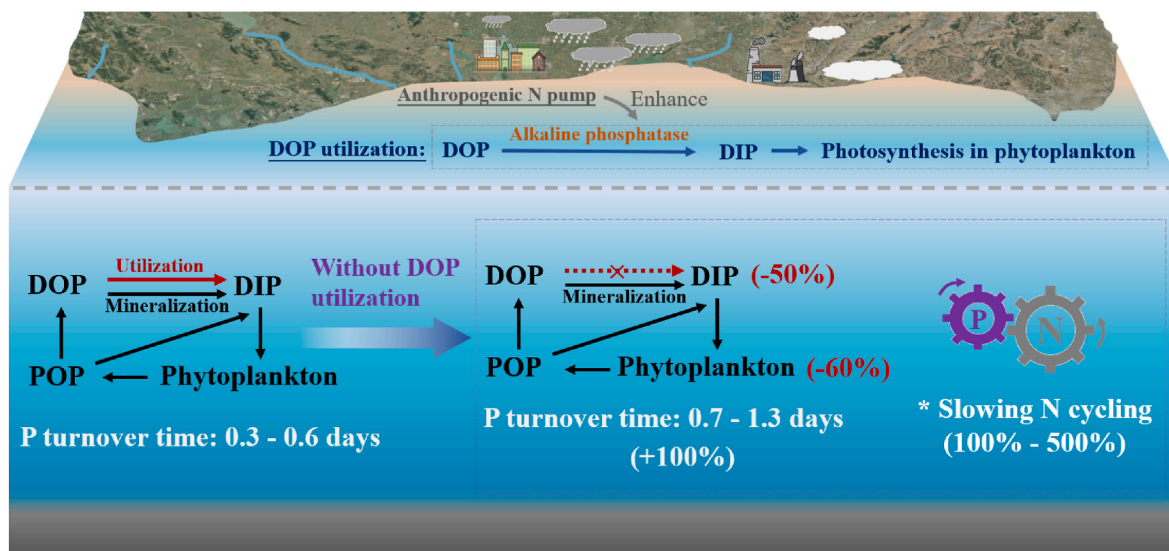

Fig. 6. Schematic representation of the role of DOP utilization parameterization in affecting phytoplankton growth, phosphorus and nitrogen cycling.

physical transport processes. Despite these methodological constraints, our approach remains a valid and practical way to quantify DOP utilization and its role in P cycling under P-limited conditions.

Several alternative techniques, such as ^{31}P nuclear magnetic resonance spectroscopy (^{31}P NMR) and radioactive phosphorus isotopes (^{32}P, ^{33}P), have been employed to investigate phosphorus transformations in marine environments (Sokoll et al., 2017; Defforey and Paytan, 2018). However, their application in directly quantifying DOP utilization rates remains limited. In particular, the radiotracer method using ^{33}P-ATP primarily reflects the turnover of labile DOP compounds rather than the total DOP pool, making it unsuitable for assessing bulk DOP utilization (M. Nausch and G. Nausch, 2006). Given these

limitations, our APA-based approach offers a viable alternative for obtaining high-resolution estimates of DOP utilization rates in coastal waters. While APA does not directly quantify absolute DOP utilization rates, this method enables a more comprehensive understanding of the dynamic nature of P cycling, which remains difficult to achieve using conventional experimental techniques.

The DIP threshold is a critical factor controlling DOP utilization, with substantial variations observed across different coastal systems. For instance, the DIP threshold is 0.03 mmol m^{-3} in the South China Sea and the Sargasso Sea (Mclaughlin et al., 2013; Chu et al., 2018), while it can reach up to 0.2 mmol m^{-3} in the Baltic Sea and Daya Bay (Nausch et al., 1998; Zhang et al., 2018). These variations can be influenced by

complex environmental factors, including cell abundance, sea temperature, and pH (Dyhrman and Kathleen, 2006; Browning et al., 2017; Jin et al., 2024). The parameterization scheme developed in this study is based on a DIP threshold of 0.02 mmol m^{-3} specific to the Yellow Sea and may not apply directly to regions with significantly different DIP thresholds. However, the methodology and functional forms used in this parameterization can provide valuable insights for quantifying DOP utilization rates in other coastal areas. In particular, the established scheme may be particularly useful for coastal regions with similar nutrient environments. For example, the summertime DIP threshold is also 0.02 mmol m^{-3} in the Bohai Sea, where environmental characteristics resemble those of the Yellow Sea (Jin et al., 2024). Preliminary calculations suggest that spatiotemporal variations in DOP utilization rates in the Bohai Sea follow a similar pattern, with significantly higher values in spring and summer compared to other seasons (Fig. 4). These findings suggest that our parameterization scheme could serve as a useful tool for understanding DOP dynamics in other P-limited coastal ecosystems.

4. Conclusions

Based on 14 incubation experiments conducted in the Yellow Sea, we quantified the negative correlation between the DOP utilization rate and DIP concentration, along with the positive effect of DIN concentration on DOP utilization when DIP concentration was below 0.02 mmol m^{-3}. A parameterization scheme for the DOP utilization rate was further developed, which effectively illustrates the distinct spatiotemporal variations in surface DOP utilization across the Yellow Sea. The incorporation of this parameterization into an ecological model enhances its ability to simulate daily nutrient cycling under varying nutrient scenarios. Model results indicate that excluding DOP utilization leads to reductions of over 50% in both DIP and Chl-a concentrations. while simultaneously doubling P and N turnover times, thereby substantially altering nutrient cycling dynamics.

While our findings provide valuable insights into DOP utilization and its role in nutrient cycling, further research is needed to validate and refine the proposed parameterization. Future studies could integrate field-based isotopic tracer techniques and in situ mesocosm experiments to directly quantify DOP utilization rates across diverse coastal environments. Additionally, larger-scale incubation experiments and long-term biogeochemical monitoring, coupled with phytoplankton community analyses, could improve our understanding of the regulatory mechanisms controlling DOP utilization under varying nutrient regimes. Given the potential influence of physical transport processes and the extended retention time of active alkaline phosphatase in seawater (Davis and Mahaffey, 2017; Thomson et al., 2019), coupling hydrodynamic-biogeochemical models with empirical datasets may offer a more comprehensive framework for evaluating DOP turnover in dynamic coastal systems.

Expanding the spatial and temporal coverage of DOP utilization measurements, particularly in other P-limited coastal regions, could further validate the robustness of our parameterization scheme. Such efforts would not only enhance our understanding of DOP dynamics but also provide critical insights for refining marine ecological models and informing coastal nutrient management strategies.

CRediT authorship contribution statement

Xiaokun Ding: Writing – original draft. **Haoyu Jin:** Writing – original draft. **Chao Zhang:** Writing – review & editing. **Lei Lin:** Data curation. **Xinyu Guo:** Methodology. **Aobo Wang:** Validation. **Jie Shi:** Resources. **Xiaohong Yao:** Conceptualization. **Huiwang Gao:** Methodology.

Declaration of competing interest

The authors declare that they have no known competing financial interests or personal relationships that could have appeared to influence the work reported in this paper.

Appendix A. Supplementary data

Supplementary data to this article can be found online at https://doi.org/10.1016/j.envpol.2025.125902.

Data availability

The data used in this study are available upon request to the corresponding author.

References

Bell, D.W., Pellechia, P.J., Ingall, E.D., Benitez-Nelson, C.R., 2020. Resolving marine dissolved organic phosphorus (DOP) composition in a coastal estuary. Limnol. Oceanogr. 65 (11), 2787–2799.

Benitez-Nelson, C.R., Buesseler, K.O., 1999. Variability of inorganic and organic phosphorus turnover rates in the coastal ocean. Nature 398 (6727), 502–505.

Benitez-Nelson, C.R., 2000. The biogeochemical cycling of phosphorus in marine systems. Earth Sci. Rev. 51 (1), 109–135.

Björkman, K.M., Duhamel, S., Church, M.J., Karl, D.M., 2018. Spatial and temporal dynamics of inorganic phosphate and adenosine-5′-triphosphate in the North Pacific Ocean. Front. Mar. Sci. 5.

Browning, T.J., Achterberg, E.P., Yong, J.C., Rapp, I., Utermann, C., Engel, A., Moore, C. M., 2017. Iron limitation of microbial phosphorus acquisition in the tropical North Atlantic. Nat. Commun. 8 (1), 15465.

Casey, J.R., Lomas, M.W., Michelou, V.K., Dyhrman, S.T., Orchard, E.D., Ammerman, J. W., Sylvan, J.B., 2009. Phytoplankton taxon-specific orthophosphate (Pi) and ATP utilization in the western subtropical North Atlantic. Aquat. Microb. Ecol. 58 (1), 31–44.

Chen, B., Liu, H., 2010. Relationships between phytoplankton growth and cell size in surface oceans: interactive effects of temperature, nutrients, and grazing. Limnol. Oceanogr. 55 (3), 965–972.

Cheung, S., Liu, K., Turk-Kubo, K.A., Nishioka, J., Suzuki, K., Landry, M.R., Zehr, J.P., Leung, S., Deng, L., Liu, H., 2022. High biomass turnover rates of endosymbiotic nitrogen-fixing cyanobacteria in the western Bering Sea. Limnology and Oceanography Letters 7 (6), 501–509.

Chu, Q., Liu, Y., Shi, J., Zhang, C., Gong, X., Yao, X.H., Guo, X.Y., Gao, H.W., 2018. Promotion effect of asian dust on phytoplankton growth and potential dissolved organic phosphorus utilization in the South China sea. J. Geophys. Res.: Biogeosciences 123 (3), 1101–1116.

Davies, A.G., Smith, M.A., 1988. Alkaline phosphatase activity in the western English Channel. J. Mar. Biol. Assoc. U. K. 68 (2), 239–250.

Davis, C.E., Mahaffey, C., 2017. Elevated alkaline phosphatase activity in a phosphate-replete environment: influence of sinking particles. Limnol. Oceanogr. 62 (6), 2389–2403.

Defforey, D., Paytan, A., 2018. Phosphorus cycling in marine sediments: advances and challenges. Chem. Geol. 477, 1–11.

Diaz, J.M., Holland, A., Sanders, J.G., Bulski, K., Mollett, D., Chou, C., Phillips, D., Tang, Y., Duhamel, S., 2018. Dissolved organic phosphorus utilization by phytoplankton reveals preferential degradation of polyphosphates over phosphomonoesters. Front. Mar. Sci. 5.

Ding, X., Li, X., Wang, A., Guo, X., Xu, X., Liu, C., Qin, X., Xie, Y., Wei, Y., Cui, Z., Jiang, T., 2024. Unprecedented phytoplankton blooms in autumn/winter in the southern Bohai Sea (China) due to high Yellow River discharge: implications of extreme rainfall events. J. Environ. Manag. 351, 119901.

Ding, X.K., Guo, X.Y., Gao, H.W., Gao, J., Shi, J., Yu, X.J., Wu, Z.S., 2021. Seasonal variations of nutrient concentrations and their ratios in the central Bohai Sea. Sci. Total Environ. 799, 149416.

Duhamel, S., Diaz, J.M., Adams, J.C., Djaoudi, K., Steck, V., Waggoner, E.M., 2021. Phosphorus as an integral component of global marine biogeochemistry. Nat. Geosci. 14 (6), 359–368.

Dyhrman, S.T., Ruttenberg, K.C., 2006. Presence and regulation of alkaline phosphatase activity in eukaryotic phytoplankton from the coastal ocean: implications for dissolved organic phosphorus remineralization. Limnol. Oceanogr. 51 (3), 1381–1390.

Eppley, R.W., 1971. Temperature and phytoplankton growth in the sea. Fish. Bull. 4 (70), 1063.

Fan, W., Song, J.B., 2014. A numerical study of the seasonal variations of nutrients in the Changjiang River estuary and its adjacent sea area. Ecol. Model. 291, 69–81.

Fang, W., Geng, B., Xiu, P., 2022. Typhoon effects on the vertical chlorophyll distribution on the northern shelf of the South China sea. J. Geophys. Res.: Oceans 127 (12).

Fennel, K., Wilkin, J., Levin, J., Moisan, J., O'Reilly, J., Haidvogel, D., 2006. Nitrogen cycling in the Middle Atlantic Bight: results from a three-dimensional model and implications for the North Atlantic nitrogen budget. Glob. Biogeochem. Cycles 20 (3).

Fitzsimons, M.F., Probert, I., Gaillard, F., Rees, A.P., 2020. Dissolved organic phosphorus uptake by marine phytoplankton is enhanced by the presence of dissolved organic nitrogen. J. Exp. Mar. Biol. Ecol. 530–531, 151434.

Gao, G., Yang, D., Xu, L., Zhang, K., Feng, X., Yin, B., 2022. A biological-parameter-optimized modeling study of physical drivers controlling seasonal chlorophyll blooms off the southern coast of Java Island. J. Geophys. Res.: Oceans.

Ghyoot, C., Gypens, N., Flynn, K.J., Lancelot, C., 2015. Modelling alkaline phosphatase activity in microalgae under orthophosphate limitation: the case of Phaeocystis globosa. J. Plankton Res. 37 (5), 869–885.

Hopkinson, C.S., Vallino, J.J., Nolin, A., 2002. Decomposition of dissolved organic matter from the continental margin. Deep Sea Res. Part II Top. Stud. Oceanogr. 49 (20), 4461–4478.

Hoppe, H., 1983. Significance of exoenzymatic activities in the ecology of brackish water: measurements by means of methylumbelliferyl-substrates. Mar. Ecol. Prog. Ser. 11 (3), 299–308.

Hung, J.J., Chen, C.H., Gong, G.C., Sheu, D.D., Shiah, F.K., 2003. Distributions, stoichiometric patterns and cross-shelf exports of dissolved organic matter in the East China Sea. Deep Sea Res. Part II Top. Stud. Oceanogr. 50 (6), 1127–1145.

Ivančić, I., Pfannkuchen, M., Godrijan, J., Djakovac, T., Marić Pfannkuchen, D., Korlević, M., Gašparović, B., Najdek, M., 2016. Alkaline phosphatase activity related to phosphorus stress of microphytoplankton in different trophic conditions. Prog. Oceanogr. 146, 175–186.

Jin, H., Zhang, C., Meng, S., Wang, Q., Ding, X., Meng, L., Zhuang, Y., Yao, X., Gao, Y., Shi, F., Mock, T., Gao, H., 2024. Atmospheric deposition and river runoff stimulate the utilization of dissolved organic phosphorus in coastal seas. Nat. Commun. 15 (1).

Jin, J., Liu, S., Ren, J., 2021. Phosphorus utilization by phytoplankton in the Yellow Sea during spring bloom: cell surface adsorption and intracellular accumulation. Mar. Chem. 231, 103935.

Karl, D.M., 2014. Microbially mediated transformations of phosphorus in the sea: new views of an old cycle. Ann. Rev. Mar. Sci (6), 279–337.

Kremer, C.T., Thomas, M.K., Litchman, E., 2017. Temperature- and size-scaling of phytoplankton population growth rates: reconciling the Eppley curve and the metabolic theory of ecology. Limnol. Oceanogr. 62 (4), 1658–1670.

Laurent, A., Fennel, K., Hu, J., Hetland, R., 2012. Simulating the effects of phosphorus limitation in the Mississippi and Atchafalaya River plumes. Biogeosciences 9 (11), 4707–4723.

Letscher, R.T., Moore, J.K., 2015. Preferential remineralization of dissolved organic phosphorus and non-Redfield DOM dynamics in the global ocean: impacts on marine productivity, nitrogen fixation, and carbon export. Glob. Biogeochem. Cycles 29 (3), 325–340.

Li, M., Liu, J., Wang, J., Song, Z., Bouwman, A.F., Ran, X., 2024. Phosphorus depletion is exacerbated by increasing nitrogen loading in the Bohai sea. Environ. Pollut. 352, 124119.

Liang, Z., Letscher, R.T., Knapp, A.N., 2022. Dissolved organic phosphorus concentrations in the surface ocean controlled by both phosphate and iron stress. Nat. Geosci. 15 (8), 651–657.

Lin, S., Litaker, R.W., Sunda, W.G., 2016. Phosphorus physiological ecology and molecular mechanisms in marine phytoplankton. J. Phycol. 52 (1), 10–36.

Liu, H., Lin, L., Wang, Y., Du, L., Wang, S., Zhou, P., Yu, Y., Gong, X., Lu, X., 2022. Reconstruction of monthly surface nutrient concentrations in the Yellow and Bohai seas from 2003–2019 using machine learning. Remote Sens. 14 (19), 5021.

Llebot, C., Spitz, Y.H., Solé, J., Estrada, M., 2010. The role of inorganic nutrients and dissolved organic phosphorus in the phytoplankton dynamics of a Mediterranean bay. J. Mar. Syst. 83 (3–4), 192–209.

Lomas, M.W., Burke, A.L., Lomas, D.A., Bell, D.W., Shen, C., Dyhrman, S.T., Ammerman, J.W., 2010. Sargasso Sea phosphorus biogeochemistry: an important role for dissolved organic phosphorus (DOP). Biogeosciences 7 (2), 695–710.

Lu, Z., Lei, L., Lu, Y., Peng, L., Han, B., 2021. Phosphorus deficiency stimulates dominance of Cylindrospermopsis through facilitating cylindrospermopsin-induced alkaline phosphatase secretion: integrating field and laboratory-based evidences. Environ. Pollut. 290, 117946.

Mahaffey, C., Reynolds, S., Davis, C.E., Lohan, M.C., 2014. Alkaline phosphatase activity in the subtropical ocean: insights from nutrient, dust and trace metal addition experiments. Front. Mar. Sci. 1.

McLaughlin, K., Sohm, J.A., Cutter, G.A., Lomas, M.W., Paytan, A., 2013. Phosphorus cycling in the Sargasso Sea: investigation using the oxygen isotopic composition of phosphate, enzyme-labeled fluorescence, and turnover times. Glob. Biogeochem. Cycles 27 (2), 375–387.

Middelburg, J.J., Nieuwenhuize, J., 2000. Uptake of dissolved inorganic nitrogen in turbid, tidal estuaries. Mar. Ecol. Prog. Ser. 192, 79–88.

Moon, J.Y., Lee, K., Lim, W.A., Lee, E., Dai, M., Choi, Y.H., Han, I.S., Shin, K., Kim, J.M., Chae, J., 2021. Anthropogenic nitrogen is changing the East China and Yellow seas from being N deficient to being P deficient. Limnol. Oceanogr. 66 (3), 914–924.

Nausch, M., 1998. Alkaline phosphatase activities and the relationship to inorganic phosphate in the Pomeranian Bight (southern Baltic Sea). Aquat. Microb. Ecol. 16 (1), 87–94.

Nausch, M., Nausch, G., 2006. Bioavailability of dissolved organic phosphorus in the Baltic Sea. Mar. Ecol. Prog. Ser. 321, 9–17.

Neddermann, K., Nausch, M., 2005. Effects of organic and inorganic nitrogen compounds on the activity of bacterial alkaline phosphatase. Aquat. Ecol. 38 (4), 475–484.

Nausch, M., Achterberg, E.P., Bach, L.T., Brussaard, C.P.D., Crawfurd, K.J., Fabian, J., Riebesell, U., Stuhr, A., Unger, J., Wannicke, N., 2018. Concentrations and uptake of dissolved organic phosphorus compounds in the Baltic Sea. Front. Mar. Sci. 5.

Ou, L., Liu, X., Li, J., Qin, X., Cui, L., Lu, S., 2018. Significant activities of extracellular enzymes from a brown tide in the coastal waters of Qinhuangdao, China. Harmful Algae 74, 1–9.

Prasad, M.B.K., Sapiano, M.R.P., Anderson, C.R., Long, W., Murtugudde, R., 2010. Long-term variability of nutrients and chlorophyll in the Chesapeake Bay: a retrospective analysis, 1985–2008. Estuaries Coasts 33 (5), 1128–1143.

Rees, A.P., Hope, S.B., Widdicombe, C.E., Dixon, J.L., Woodward, E.M.S., Fitzsimons, M.F., 2009. Alkaline phosphatase activity in the western English Channel: elevations induced by high summertime rainfall, Estuarine. Coastal and Shelf Science 81 (4), 569–574.

Ruttenberg, K.C., Dyhrman, S.T., 2005. Temporal and spatial variability of dissolved organic and inorganic phosphorus, and metrics of phosphorus bioavailability in an upwelling-dominated coastal system. J. Geophys. Res.: Oceans 110 (C10).

Ruttenberg, K.C., Dyhrman, S.T., 2012. Dissolved organic phosphorus production during simulated phytoplankton blooms in a coastal upwelling system. Front. Microbiol. 3.

Shen, Y., Wang, W.L., 2025. Autotrophic dissolved organic phosphorus uptake stimulates nitrogen fixation in subtropical gyres. Geophys. Res. Lett. 52 (2).

Shukla, J.B., Arora, M.S., Verma, M., Misra, A.K., Takeuchi, Y., 2021. The impact of sea level rise due to global warming on the coastal population dynamics: a modeling study. Earth Systems and Environment.

Sisma-Ventura, G., Rahav, E., 2019. DOP stimulates heterotrophic bacterial production in the oligotrophic southeastern mediterranean coastal waters. Front. Microbiol. 10.

Sokoll, S., Ferdelman, T.G., Holtappels, M., Goldhammer, T., Littmann, S., Iversen, M.H., Kuypers, M.M.M., 2017. Intense biological phosphate uptake onto particles in subeuphotic continental margin waters. Geophys. Res. Lett. 44 (6), 2825–2834.

Su, B., Song, X., Duhamel, S., Mahaffey, C., Davis, C., Ivančić, I., Liu, J., 2023. A dataset of global ocean alkaline phosphatase activity. Sci. Data 10 (1), 205.

Suzumura, M., Hashihama, F., Yamada, N., Kinouchi, S., 2012. Dissolved phosphorus pools and alkaline phosphatase activity in the euphotic zone of the western north pacific ocean. Front. Microbiol. 3.

Thomson, B., Wenley, J., Currie, K., Hepburn, C., Herndl, G.J., Baltar, F., 2019. Resolving the paradox: continuous cell-free alkaline phosphatase activity despite high phosphate concentrations. Mar. Chem. 214, 103671.

Wang, D., Huang, B., Liu, X., Liu, G., Wang, H., 2014. Seasonal variations of phytoplankton phosphorus stress in the Yellow Sea cold water mass. Acta Oceanol. Sin. 33 (10), 124–135.

Wang, Q., Zhang, C., Jin, H., Chen, Y., Yao, X., Gao, H., 2022. Effect of anthropogenic aerosol addition on phytoplankton growth in coastal waters: role of enhanced phosphorus bioavailability. Front. Microbiol. 13.

Wang, Y.C., Guo, X.Y., Zhao, L., 2018. Simulating the responses of a low-trophic ecosystem in the East China Sea to decadal changes in nutrient load from the Changjiang (Yangtze) River. Journal of Oceanology and Limnology 36 (1), 48–61.

Wang, Z., Liang, Y., Kang, W., 2011. Utilization of dissolved organic phosphorus by different groups of phytoplankton taxa. Harmful Algae 12, 113–118.

Xiu, P., Chai, F., 2021. Impact of atmospheric deposition on carbon export to the deep ocean in the subtropical northwest Pacific. Geophys. Res. Lett. 48 (6).

Yoshikawa, C., Yamanaka, Y., Nakatsuka, T., 2005. An ecosystem model including nitrogen isotopes: perspectives on a study of the. Marine Nitrogen Cycle 61 (5), 921–942.

Yoshikawa, C., Abe, H., Aita, M.N., Breider, F., Kuzunuki, K., Toyoda, S., Ogawa, N.O., Suga, H., Ohkouchi, N., Danielache, S.O., Wakita, M., Honda, M.C., Yoshida, N., 2015. Insight into nitrous oxide production processes in the western North Pacific based on a marine ecosystem isotopomer model. J. Oceanogr. 72 (3), 491–508.

Yu, L.Q., Gan, J.P., Dai, M.H., Hui, C.R., Lu, Z.M., Li, D., 2021. Modeling the role of riverine organic matter in hypoxia formation within the coastal transition zone off the Pearl River Estuary. Limnol. Oceanogr. 66 (2), 452–468.

Zhang, J., Guo, X., Zhao, L., 2019. Tracing external sources of nutrients in the East China Sea and evaluating their contributions to primary production. Prog. Oceanogr. 176, 102122.

Zhang, X., Zhang, J., Shen, Y., Zhou, C., Huang, X., 2018. Dynamics of alkaline phosphatase activity in relation to phytoplankton and bacteria in a coastal embayment Daya Bay, South China. Mar. Pollut. Bull. 131, 736–744.

Zhang, Y.H., Yin, M.R., 2007. Phosphorus cycling in the upper ocean of the East China Sea using natural 32P and 33P. Acta Oceanol. Sin. 1, 49–57 (In Chinese with English abstract).

Zhou, J., Chai, F., Huang, D., Xue, H., Chen, J., Xiu, P., Xuan, J., Li, J., Zeng, D., Ni, X., Wang, K., 2017. Investigation of hypoxia off the Changjiang Estuary using a coupled model of ROMS-CoSiNE. Prog. Oceanogr. 159, 237–254.

Zhong, X., Ran, X., 2024. Deciphering and quantifying nitrate sources and processes in the central Yellow Sea using dual isotopes of nitrate. Water Res. 261, 121995.

Zhou, L., Liu, F., Liu, Q., Fortin, C., Tan, Y., Huang, L., Campbell, P.G.C., 2021. Aluminum increases net carbon fixation by marine diatoms and decreases their decomposition: evidence for the iron–aluminum hypothesis. Limnol. Oceanogr. 66 (7), 2712–2727.

Zhu, J., Shi, J., Guo, X., Gao, H., Yao, X., 2018. Air-sea heat flux control on the Yellow Sea Cold Water Mass intensity and implications for its prediction. Cont. Shelf Res. 152, 14–26.